sciendo

POLISH MARITIME RESEARCH 2 (102) 2019 Vol. 26; pp. 55-67
10.2478/pomr-2019-0025

METHOD OF EMERGENCY COLLISION AVOIDANCE FOR UNMANNED SURFACE VEHICLE (USV) BASED ON MOTION ABILITY DATABASE

Lifei Song[1, 2]
Houjing Chen[1, 3]
Wenhao Xiong[2]
Zaopeng Dong[2]
Puxiu Mao[4]
Zuquan Xiang[2]
Kai Hu[3]

[1] Key Laboratory of High Performance Ship Technology (Wuhan University of Technology), Ministry of Education, Wuhan, China
[2] School of Transportation, Wuhan University of Technology, China
[3] China Ship Development and Design Center, Wuhan, China
[4] University of Southern California, Los Angeles, USA

ABSTRACT

The unmanned surface vehicles (USV) are required to perform a dynamic obstacle avoidance during fulfilling a task. This is essential for USV safety in case of an emergency and such action has been proved to be difficult. However, little research has been done in this area. This study proposes an emergency collision avoidance algorithm for unmanned surface vehicles (USVs) based on a motion ability database. The algorithm is aimed to address the inconsistency of the existing algorithm. It is proposed to avoid collision in emergency situations by sharp turning and treating the collision avoidance process as a part of the turning movement of USV. In addition, the rolling safety and effect of speed reduction during the collision avoidance process are considered. First, a USV motion ability database is established by numerical simulation. The database includes maximum rolling angle, velocity vector, position scalar, and steering time data during the turning process. In emergency collision avoidance planning, the expected steering angle is obtained based on the International Regulations for Preventing Collisions at Sea (COLREGs), and the solution space, with initial velocity and rudder angle taken as independent variables, is determined by combining the steering time and rolling angle data. On the basis of this solution space, the objective function is solved by the particle swarm optimization (PSO) algorithm, and the optimal initial velocity and rudder angle are obtained. The position data corresponding to this solution is the emergency collision avoidance trajectory. Then, the collision avoidance parameters were calculated based on the afore mentioned model of motion. With the use of MATLAB and Unity software, a semi-physical simulation platform was established to perform the avoidance simulation experiment under emergency situation. Results show the validity of the algorithm. Hence results of this research can be useful for performing intelligent collision avoidance operations of USV and other autonomous ships

Keywords: Unmanned surface vehicle; emergency collision avoidance; velocity obstacle method; motion ability

INTRODUCTION

An unmanned surface vehicle (USV) is a ship that navigates on water in an autonomous manner. Its autonomous collision avoidance capability is the basis for safe navigation and undertaking maritime tasks. Autonomous obstacle avoidance skill is the foundation for executing tasks and also the reflection of its intelligence [1, 2].

The International Maritime Organization (IMO) approved the International Regulations for Preventing Collisions at Sea (COLREGS) in 1972 [3]. The regulations specify certain rules of navigation for ships at risk of collision. During collision avoidance action USVs should follow the regulations and assume that the obstacles (obstacle boats in this article) comply with the regulations, which has become the consensus for research on intelligent collision avoidance [4].

On this premise, various algorithms have been proposed in many studies. The artificial potential field [8] is one of them. The path planned by this method is smooth and safe, but the method also falls into the local optimal solution. In most

studies the local optimal solution are avoided through manual interference and correction, but the effect is not good when multiple obstacles are present [9–10].

Evolutionary algorithms [5] include several methods which are all-population optimization algorithms taking individuals as optional paths. The optimization of the collision avoidance paths is carried out along with the evolution of the population. The above-mentioned population evolution methods generally establish the path model in two ways. As shown in Fig. 2, the first one is 2-D grid maps [6, 7] where the obstacle space and free space are determined by coordinates, and the other one consists in establishing a path model according to the individual size of the population. The map of the path model can be further divided into that Cartesian coordinates-based and that polar coordinates-based.

Regardless of which of the above coordinate systems is used, each alternative path is represented as an individual in the population. The length and smoothness of the path polyline is used as a measure of the fitness function during the population optimization. The alternative paths are evolved by internal operators such as selection, crossover and mutation.

However, the population evolution methods have three disadvantages. First, the methods require a large amount of data and lead to a high computation cost; furthermore, the evolutionary process of individuals lacks regularity when they are represented by paths, which makes it difficult to find problems when unreasonable number of iterations occur. Second, in the case of dynamic collision avoidance, the continuous motion of obstacles makes the environmental information varying in time, but as any change is not considered in these methods a low intelligence in collision avoidance actions is produced. Third, the motion of multiple obstacles is represented simply by the change in 2D grid coordinates, hence the comprehensive impact of obstacles on collision avoidance process cannot be included, which leads to unsatisfactory results in emergency dynamic avoidance situation.

The velocity obstacle (VO) approach was first introduced in the robotics field [11]. The VO method forms a cone-shaped space on the obstacle, and ensures that the USV never collides with the obstacle if it remains outside the space. Extensive research on the velocity obstacle approach has been conducted in collision avoidance planning for unmanned surface vehicles [12–14]. The fast computing capability of the algorithm ensures a quick reaction of robots. However, for a USV which moves at a high speed, the avoidance effect against dynamic obstacles is difficult to ensure in complex circumstances. Thus, it is mainly used under relatively safe conditions. Neural networks [15] have also been widely studied in collision avoidance issues. An algorithm which uses a neural network exhibits fast convergence and good adaptability, but it considers all inference processes as numerical calculations, thereby leading to poor generalization and falling into local optima, especially under the condition of dynamic collision avoidance of multiple obstacles, where the feasible space is narrow and the environment changes in real time, and a relatively high accuracy and real-time performance in collision avoidance process is required. Therefore, the application of this method is limited in practical maritime navigation.

Moreover, existing research focuses mainly on situations in which the movements of obstacles do not pose an extreme threat to the USV. Therefore, when the obstacles do not follow the COLREGS and lead to an urgent situation, the afore mentioned algorithms may fail.

In emergency case of collision avoidance, the above mentioned algorithms are rarely used mainly due to the following reasons [16–17]:

(1) The collision avoidance strategy is non-continuous. In the case of dynamic collision avoidance, the continuous motion of obstacles makes the environmental information varying in time, but as any change is not considered in these methods, a low intelligence in collision avoidance actions is produced. The existing collision-avoidance algorithms, such as the VO algorithm, adjust only the motion based on the information at current time, that leads to a lack of prediction about the movement of both the USV and the obstacles, thereby also to an incoherence of the algorithm in obstacle avoidance problems and making the USV to move along a zigzag trajectory. In addition, the course of a USV must be sharply adjusted in an emergency situation, which may lead to a lack of a solution complying with the principle of the VO algorithm.

(2) The relationship between velocity and position is nonlinear. Fig. 1 shows the relationship between instantaneous velocity and position. The green arrow in the figure stands for the velocity vector and the blue arrow for the actual position vector. In non-emergency collision avoidance situation, as shown in Fig. 1(a) and given by Eq. (1), position and velocity have a linear relationship. The above mentioned algorithms estimate mainly the collision risk based on the following relationship:

$$\boldsymbol{p}(t) = \boldsymbol{p}(t-1) + \boldsymbol{v}(t) \tag{1}$$

where, $\boldsymbol{p}(t)$ is the position vector at time t, $\boldsymbol{v}(t)$ is the velocity vector at time t.
In the case of large-range steering, as shown in Fig. 1(b), the course of the USV significantly changes during one cycle, and the relationship between position and velocity is nonlinear. Consequently, the position is difficult to approximate by using the velocity vector.

(3) The effect of ship heeling on its safety is not considered. The current research generally does not consider the heel of USV. However, in an emergency situation the large turn of the USV produces a large heel angle that may cause the USV to capsize.

(4) The influence of speed reduction is not considered. The speed may be reduced when the USV sharply turns to avoid collision, and the speed reduction extent varies with the initial speed and rudder angle. If speed reduction is not considered during collision avoidance action, collision may occur during actual execution of the action in a result

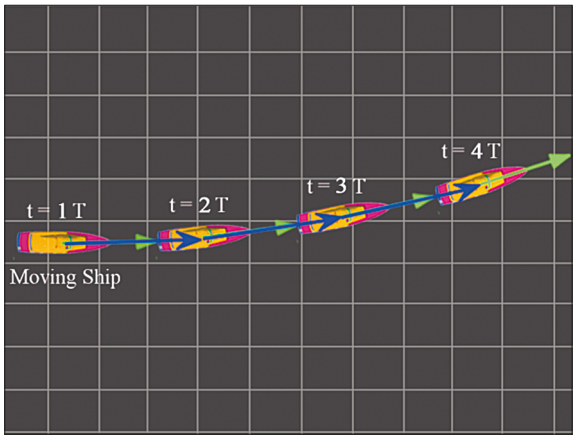

(a) Rarely changing course

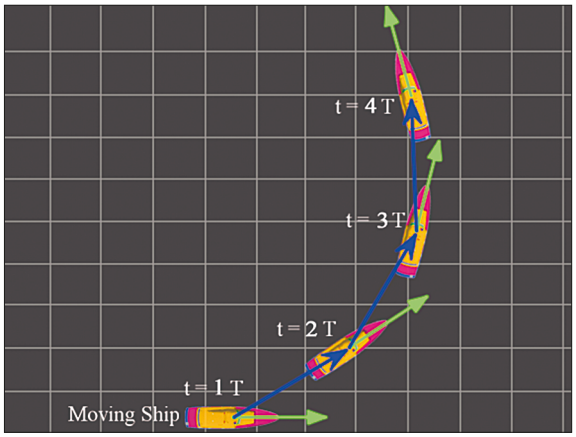

(b) Significantly changing course

Fig. 1. Relationship between position and velocity of a ship

of the decrease of speed, otherwise the USV engine must be forced to speed up for safety [18–20].

In view of the preceding deficiencies, the collision avoidance movement of USVs should have the following characteristics in an emergency situation:

(1) Priority should be given to adjusting the course. Course adjustment has a better effect than speed adjustment, and a change in course is easier to be recognized by other ships enabling them to adjust their motions, accordingly [21].

(2) Given the speed reduction and heeling problem, collision avoidance planning should be established based on the dynamics of USVs to ensure that the planned trajectory can be tracked easily.

(3) Avoidance operations should be continuous. Frequent adjustments delay avoidance action in emergency situations. Therefore, correct collision avoidance planning should be conducted at the beginning and implemented thereafter.

According to the above presented analysis, in urgent situations, the optimal collision avoidance operation should include consistent steering the rudder to a certain angle to alter the direction of the USV to avoid obstacles. Meanwhile, the speed and heading are continuously fine tuned. This obstacle avoidance process can be simplified as a part of the turning motion. This paper proposes an algorithm based on the motion ability database of USVs for collision avoidance in emergency situations.

The paper is organized as follows. In Section 1, the motion ability database of the USV was established by simulation. In Section 2, the positional relationship model between USV and obstacles was established and the classification of the collision risk carried out. In Section 3, the collision avoidance strategy and solution method are defined. In Section 4, simulations of trajectory prediction and obstacle avoidance are carried out, and their results are analyzed in detail to verify the effectiveness of the algorithm. In Section 5, the recapitulation of the study is offered.

ESTABLISHING AN USV POWER DATABASE

ANALYSIS OF USV MOTION CHARACTERISTICS

A dynamic model is established for USVs by using the separate model structure (MMG, Ship Manoeuvring Mathematical Model Group), and the state equation is solved by means of the fourth-order Runge–Kutta method. The rotary motion of a USV is analyzed in terms of rigid body mechanics. USVs use propeller propulsion, and propeller speed and rudder angle are the dynamic control parameters. The basic parameters of USVs are shown in Tab. 1.

Tab. 1. Basic parameters of unmanned boats

Term	Symbol	Unit	Value
Design length of waterline	L	m	8.2
Design width of waterline	B	m	2.3
Average draught	d	m	0.71
Drainage volume	∇	m^3	5.54
Displacement	Δ	t	5.69
Initial velocity	V_0	m/s	5
Safe heel angle		Deg	30

The trajectory of the vessel under different rudder angles at the same initial speed of 5 m/s is shown in Fig. 2. In all cases the start points and simulation time periods of 50 sec are the same. The trajectories indicate that the larger the rudder angle the smaller the turning diameter. When the rudder angle reaches 35°, the constant turning diameter is 24 m, which is approximately three times greater than the length of the boat, which indicates a good turning performance to avoid obstacles. When the rudder angle is small, e.g. 5°, the constant turning diameter is more than 200 m, which shows an insufficient manoeuvrability.

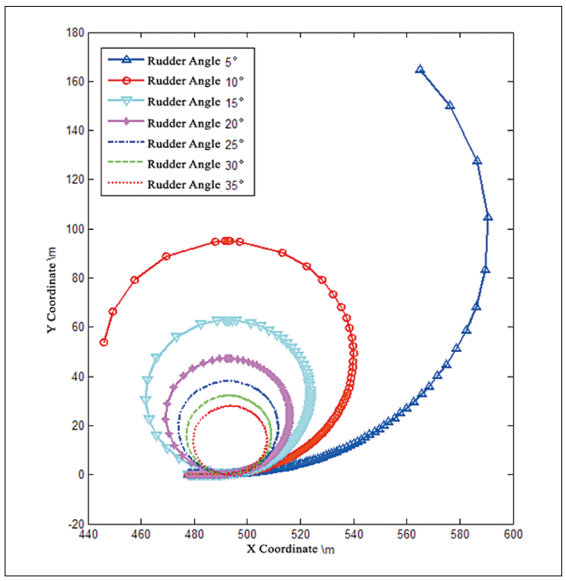

Fig. 2. USV motion track within 50 sec steering period at initial speed of 5 m/s

Fig. 3 shows the heeling angle curves for the boat at different rudder angles at the initial speed of 5 m/s. The heel angle tends to be stable at approximately 15 sec, its value is stable and relatively small due to the low speed of 5 m/s. However, prior to this condition, the maximum heel angle value is large and the rolling curves oscillate 1–2 times because of the rapidly increasing hydrodynamic force during the steering process and the quick occurrence of the camber moment. The simulation shows that a high-speed rotation produces much larger heel angle than that at a low speed, and the maximum heel angle is much larger than the steady heel angle, which is consistent with the theoretical analysis. Sailing at a high speed, USVs are often steered at a large rudder angle to avoid collision, which may cause the vehicles to roll over or overturn.

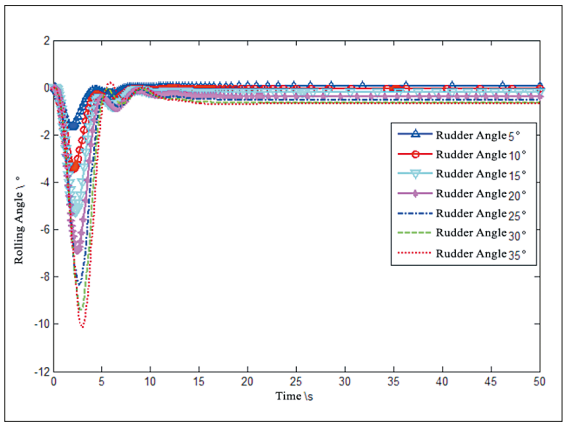

Fig. 3. USV rolling angle curves for different rudder angles at the initial speed of 5 m/s

Fig. 4 shows the speed drop curve during the rotation of the boat. The steering inevitably causes a drop in speed. When turning at a large rudder angle, the speed drop can reach 40% of the initial speed because the drift angle gradually increases with the steering angle thereby resulting in an increase in resistance against forward motion. Meanwhile, the thrust of the propeller is also consumed by the forward direction component of the centrifugal force and the rotational process changes the working conditions of the propeller, resulting in the decline of the rotational speed and efficiency and significant decrease of the forward speed.

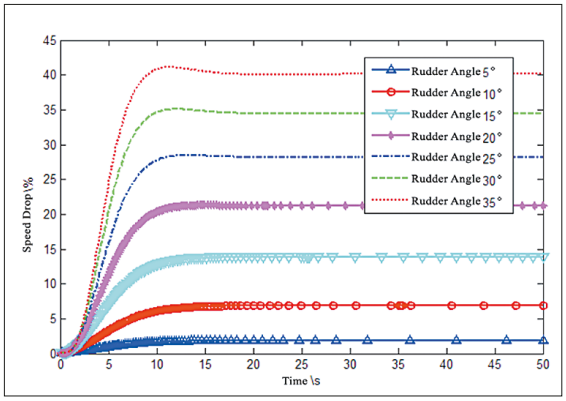

Fig. 4. USV rolling angle curves for different rudder angles at the initial speed of 5 m/s

The main data of the simulation at different rudder angles and the initial speed of 5 m/s are listed in Tab. 2. At this speed, when the rudder angle is below 10°, the heel and speed drop are also small. If the speed must be maintained while steering, the rotational speed of the main engine should be increased slightly. The larger the rudder angle, the larger the drift angle, speed drop, and heel angle and the greater the impact on the USV collision avoidance trajectory.

Tab. 2. Main data of USV rotary motion

Initial velocity (m/s)	Rudder angle (degree)	Constant speed (m/s)	Constant rotation diameter (m)	Downhill ? (percentage)	Maximum roll angle (degree)	Constant drift angle (degree)
5	5	4.8201	195.3463	1.86%	–1.6763	1.9890
5	10	4.5744	94.0141	6.86%	–3.4655	4.1122
5	15	4.2336	61.9975	13.8%	–5.2480	6.2078
5	20	3.8712	46.7099	21.18%	–6.9001	8.2072
5	25	3.5287	37.8469	28.16%	–8.3118	10.0946
5	30	3.2191	32.0803	34.46%	–9.4037	11.8738
5	35	2.9425	28.0322	40.09%	–10.1358	13.5533

ESTABLISHING A STEERING HEEL ANGLE DATABASE FOR HEEL SAFETY

Given that the emergency obstacle avoidance movement of the USV occurs in the early stage of the rotary motion, the probability of encountering the maximum roll angle is high. The rotary motion of an USV is numerically simulated within the initial speed range from 0 to 18 m/s and rudder angle range

from 5° to 35°. The scatter data of maximum heeling angle, initial speed, and rudder angle are obtained, and then fitted by means of a polynomial expressed as follows:

$$\begin{aligned}\phi_{\max}(V_x, \delta_y) = &-3.054 + 0.7447V_x + 0.6606\delta_y \\ &- 0.04852V_x^2 - 0.1532V\delta_y - 0.02769\delta_y^2 \\ &+ 0.001591V_x^3 - 0.00398V_x^2\delta_y + 0.002558V_x\delta_y^2 \\ &+ 0.003651\delta_y^3 \end{aligned} \quad (2)$$

where, $\phi_{\max}()$ represents the function of maximum roll angle. V_x – the initial speed and δ_y – the rudder angle.

The precision parameters of the polynomial fitting are as follows: the sum of square errors is 6.831, the complex correlation coefficient (R-square) is 0.9997, the adjusted R-square is 0.9996, and the root mean square error (RMSE) is 0.359. The square error and RMSE are small, and the complex correlation coefficient and the adjusted R-square are near 1, indicating a high fitting accuracy.

The polynomial surface is shown in Fig. 5. The larger the initial speed and rudder angle, the larger the maximum heel angle of the USV. When the maximum heeling angle exceeds the safe heeling angle of the USV, the risk of collision non-avoidance is great. The curve formed by the intersection of the surface and the 30° heeling plane represents the boundary between safe heel zone and danger one.

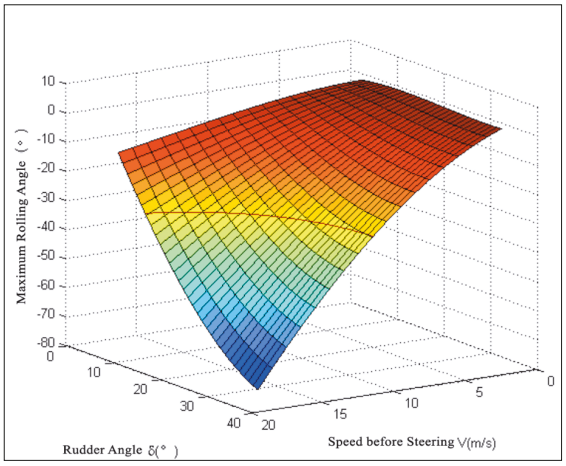

Fig. 5. Three-dimensional diagram of maximum roll angle obtained from simulation of USV turning motion

ESTABLISHING A ROTARY MOTION VELOCITY VECTOR DATABASE AND A POSITION VECTOR DATABASE

According to the numerical calculation results, the data points of the velocity vector and the position scalar in the 10 collision avoidance cycles after the start of steering, are extracted. The radar information for the boat is updated every 5 seconds, so the collision avoidance cycle is set to last 5 sec. Then, the relationships between the data and the initial velocity and between the data and the rudder angle of the USV, are established, respectively. The velocity vector is used to determine the collision avoidance direction, while the position scalar is used to determine the prediction of safety against collision.

The velocity vector database is expressed by the following equation:

$$\boldsymbol{V} = \boldsymbol{\Gamma}([\boldsymbol{U}, \boldsymbol{\delta}]) \quad (3)$$

where $\boldsymbol{\Gamma} = [\Gamma_0, \ldots, \Gamma_t, \ldots, \Gamma_{10}]^T$ is a mapping function that indicates the correspondence between the velocity vector and the initial speed and rudder angle:

$$\boldsymbol{V} = [\boldsymbol{V}_0, \ldots, \boldsymbol{V}_t, \ldots, \boldsymbol{V}_{10}]^T,$$

$$[\boldsymbol{U}, \boldsymbol{\delta}] = [(\boldsymbol{U}, \boldsymbol{\delta})|_0, \ldots (\boldsymbol{U}, \boldsymbol{\delta})|_t, \ldots (\boldsymbol{U}, \boldsymbol{\delta})|_{10}]^T$$

$$\boldsymbol{V}_t = \begin{bmatrix} \vec{V}_{0,0,t} & \cdots & \vec{V}_{0,7,t} \\ \vdots & \vec{V}_{i,j,t} & \vdots \\ \vec{V}_{19,0,t} & \cdots & \vec{V}_{19,7,t} \end{bmatrix}$$

where $t = 0,1\ldots, 9, 10$; $i = 0,1\ldots,16, 17$, stand for the index of different speeds. $j = 0,1\ldots,6, 7$,– the index of different rudder angles.

$$(\boldsymbol{U}, \boldsymbol{\delta})|_t = \begin{bmatrix} (V_0, \delta_0) & \cdots & (V_0, \delta_7) \\ \vdots & (V_i, \delta_j) & \vdots \\ (V_{19}, \delta_0) & \cdots & (V_{19}, \delta_7) \end{bmatrix}$$

UWAGA: tu i wyżej: brak objaśni symbolu U !

For example, $V_{i,j,t}$ represents the speed vector at the *t-th* turning cycle at the *i-th* initial speed and the *j-th* rudder angle (V_i, δ_j).

In collision avoidance situation, the direction of the USV must be judged through the direction information from the velocity database. During the turning motion simulation, the time required to change the speed direction by 30°, 60°, 90°, 120°, 150°, and 180° is recorded for different initial speeds and different rudder angles of the USV, For ships with a poor turning performance a denser heading angle division can be used.

The scatter data are fitted to a polynomial for easy recall. The mathematical relationship between the time required for the six steering angles, the rudder angle and the speed before steering, is expressed as follows:

$$\begin{aligned} t_\psi(V_x, \delta_y) = &\, p_{00} + p_{01}\delta_y + p_{20}V_x^2 \\ &+ p_{11}V_x\delta_y + p_{02}\delta_y^2 + p_{30}V_x^3 \\ &+ p_{21}V_x^2\delta_y + p_{12}V_x\delta_y^2 + p_{03}\delta_y^3 \\ &+ p_{40}V_x^4 + p_{31}V_x^3\delta_y + p_{22}V_x^2\delta_y^2 \\ &+ p_{13}V_x\delta_y^3 + p_{50}V_x^5 + p_{41}V_x^4\delta_y \\ &+ p_{32}V_x^3\delta_y^2 + p_{23}V_x^2\delta_y^3 \end{aligned} \quad (4)$$

where $t_\psi()$ indicates the function of the time required for different steering angles; the coefficients of each surface polynomial are shown in Tab. 3.

Tab. 3. Polynomial coefficients corresponding to target steering angle ψ

ψ (deg)	30	60	90	120	150	180
p_{00}	105.3	191.4	294.7	394	493.8	596.2
p_{10}	−33.13	−58.44	−90.96	−121	−153	−187.2
p_{01}	−8.534	−15.61	−26.02	−35.07	−43.73	−52.36
p_{20}	4.8	8.28	12.97	16.93	21.55	26.54
p_{11}	1.931	3.419	5.796	7.908	9.953	12.06
p_{02}	0.3046	0.5453	0.9616	1.289	1.587	1.874
p_{30}	−0.3653	−0.6183	−0.98	−1.243	−1.582	−1.957
p_{21}	−0.1695	−0.297	−0.4958	−0.6818	−0.8769	−1.072
p_{12}	−0.05546	−0.09564	−0.1756	−0.2381	−0.2928	−0.3476
p_{03}	−0.003715	−0.006529	−0.01199	−0.01596	−0.01939	−0.02263
p_{40}	0.01423	0.02372	0.03827	0.04693	0.05943	0.07373
p_{31}	0.006567	0.0114	0.01854	0.02551	0.03355	0.04147
p_{22}	0.003233	0.005554	0.01014	0.01393	0.01746	0.0208
p_{13}	0.000578	0.0009671	0.001895	0.002541	0.00303	0.003534
p_{50}	−0.000223	−0.000368	−0.0006045	−0.0007168	−0.0009	−0.00112
p_{41}	−9.93E−05	−0.0001686	−0.0002719	−0.0003698	−0.00049	−0.00061
p_{32}	−5.31E−05	−9.32E−05	−0.0001605	−0.0002248	−0.0003	−0.00036
p_{23}	−2.30E−05	−3.78E−05	−7.63E−05	−0.0001029	−0.00012	−0.00014

The polynomial surfaces are shown in Fig. 6. The six surfaces indicate the time required for changing the heading angle by 30°, 60°, 90°, 120°, 150°, and 180° after the start of USV steering, respectively. As the steering angle increases, the required time increases approximately in the same way. In addition, the time required to turn by the same angle at a high speed and large rudder angle is much longer than that at a low speed or small rudder angle.

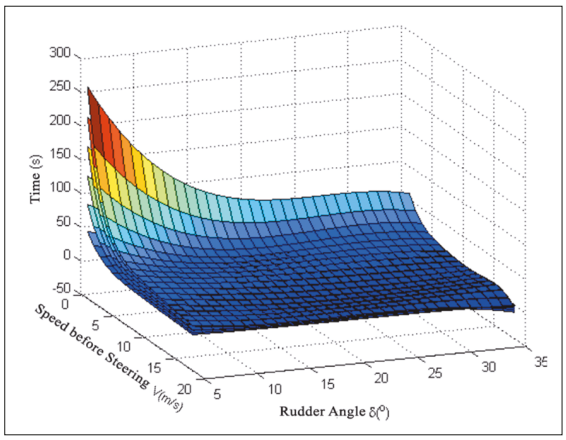

Fig. 6. Three-dimensional surface map of the time required to change the heading angle by 30°, 60°, 90°, 120°, 150°and 180°, successively

The position database is expressed as follows:

$$\boldsymbol{P} = \boldsymbol{\Lambda}([\boldsymbol{U}, \boldsymbol{\delta}]) \tag{5}$$

where $\boldsymbol{\Lambda} = [\Lambda_0, \ldots, \Lambda_t, \ldots, \Lambda_{10}]^T$ is a mapping function that indicates the correspondence between the position, the initial speed and rudder angle.

$$\boldsymbol{P} = [\boldsymbol{P}_0, \ldots, \boldsymbol{P}_t, \ldots, \boldsymbol{P}_{10}]^T,$$

$$\boldsymbol{P}_t = \begin{bmatrix} P_{0,0,t} & \cdots & P_{0,7,t} \\ \vdots & P_{i,j,t} & \vdots \\ P_{19,0,t} & \cdots & P_{19,7,t} \end{bmatrix}$$

In the above given formula, the meanings of the indices *i*, *j*, and *t*, and ($[\boldsymbol{U}, \boldsymbol{\delta}]$) are the same as those in the speed variable database. For instance,indicates the position coordinates of the USV at the *t-th* cycle when the rudder angle *j* is used for the initial speed *i*.

ESTABLISHING A COLLISION AVOIDANCE MODEL TO DETERMINE WHETHER COLLISION AVOIDANCE IS NECESSARY

JUDGMENT OF URGENCY OF USV

A low capability of error detection in the estimation and prediction of trajectories of obstacles may cause serious problems in accuracy, thereby damaging the judgment of USV and affecting the effectiveness of collision avoidance.

Considering the radar observation error to improve the prediction accuracy of the obstacle position, the prediction period $T_p(k)$ is introduced in accordance with [22] to reasonably increase the data sampling period and improve the accuracy of error elimination. Moreover, the bidirectional adaptive filtering algorithm based on polynomial fitting and particle swarm optimization [22] is used to eliminate the observed errors in ordinate and abscissa coordinates, and the trajectory of obstacle is predicted by using the autoregressive model. The value of $T_p(k)$ is given by Eq. (6):

$$T_p(k) = \left\lfloor \frac{R_w}{10 \max(\boldsymbol{v}_k)} \right\rfloor T \tag{6}$$

where R_w is the radius of the radar observation scope and T is the observation period of the radar. v_k is the relative velocity between the USV and the k-th obstacle, set for various periods, in particular, $v_k = \{v_{k,1}, v_{k,1} \ldots v_{k,n}\}$. The symbol $\lfloor x \rfloor$ indicates that the real x is rounded down. Eq. (6) shows that $T_p(k)$ is a positive integer multiple of T, and the value of T_p differs with different obstacles. $T_p(k)$ is introduced for reasonable increasing the data sampling period and improving the accuracy of error elimination.

As shown in Fig. 7, a USV with shape $\mathcal{A}$ and a moving ship with shape $\mathcal{B}$, which have velocity vectors $\mathbf{v_R}$ and $\mathbf{v_0}$, respectively, are used. The safe zone of the US is given as $\mathcal{C}$. The domain of the moving ship is $\mathcal{D}$, which is used to represent the area of an obstacle that should be avoided. The blue points in the Fig. 7 represent the obstacle position collected in the previous multiple sampling period, T. Based on the sampling coordinates and the error elimination algorithm taken from the literature, the predicted positions of the obstacle at the moment $1T_p$ and $2T_p$ are shown as **ON** and **ONN**, respectively, and the corresponding ship domains are marked $\mathcal{DN}$ and $\mathcal{DNN}$. Given the uncertainty of prediction, the domains of the $\mathcal{DN}$ and $\mathcal{DNN}$ zones are expanded. For the USV at the position P, the predicted positions in the next two T_ps are marked PN and PNN in the figure, and the corresponding safety zones are denoted by $\mathcal{CN}$ and $\mathcal{CNN}$, respectively. Given that the USV has a minimum observation error in itself, the prediction is relatively accurate and in consequence the safe zone is not expanded.

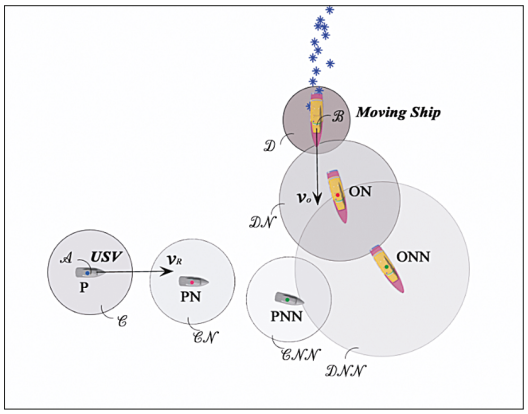

Fig. 7. Position relationship between USV and obstacle in three consecutive moments

Tab. 4. Different states of emergency situation

Symbol	Status	Description	Expected status
λ_1	$\{\mathcal{A} \cap \mathcal{B} \neq \varnothing\}$	Collision, failure to avoid collision	
λ_2	$\{\mathcal{CN} \cap \mathcal{D} \neq \varnothing\}$	Critical, must avoid collision immediately	
λ_3	$\{\mathcal{CN} \cap \mathcal{DN} \neq \varnothing\}$	Critical, must avoid collision immediately	
λ_4	$\{\mathcal{C} \cap \mathcal{DNN} \neq \varnothing\}$	Critical, must avoid collision immediately	
λ_5	$\{\mathcal{CNN} \cap \mathcal{D} \neq \varnothing\}$	Judgment is kept, collision is not avoided	Expected to enter state 2
λ_6	$\{\mathcal{CNN} \cap \mathcal{DN} \neq \varnothing\}$	Judgment is kept, collision is not avoided	Expected to enter state 3
λ_7	$\{\mathcal{C} \cap \mathcal{DNN} \neq \varnothing\}$	Judgment is kept, collision is not avoided	Expected to enter state 4
λ_8	$\{\mathcal{CN} \cap \mathcal{DNN} \neq \varnothing\}$	Judgment is kept, collision is not avoided	Expected to enter other tensions
λ_9	$\{\mathcal{CNN} \cap \mathcal{DNN} \neq \varnothing\}$	Judgment is kept, collision is not avoided	Expected to enter other tensions

In a state of emergency which can be expressed as λ_0, a strategy of collision avoidance must be introduced:

$$\lambda_0 : \lambda_2 \cup \lambda_3 \cup \lambda_4 \cup \lambda_5 \cup \lambda_6 \cup \lambda_7 \cup \lambda_8 \cup \lambda_9$$

In a state of non-emergency marked λ_{10}, the VO algorithm can be used for collision avoidance.

$$\lambda_0 : \overline{\lambda}_2 \cap \overline{\lambda}_1$$

The degree of danger at each state and the level of corresponding collision avoidance strategy are as follows:

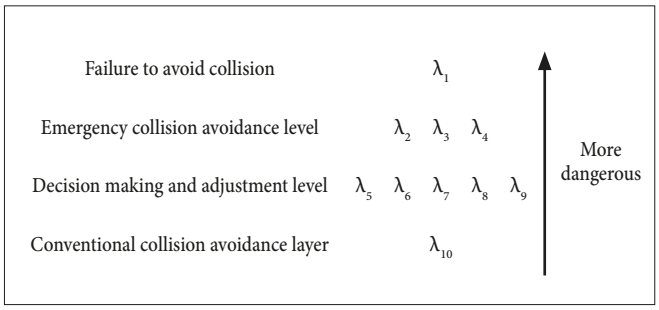

Fig. 8. Three cycles of criticality of USV and obstacle positional relation

1. **When multiple situations occur at the same time, the situation with a higher level of danger is chosen.**

With the movement of the USV and obstacle, the situation may change or the USV may be lifted from the urgent situation. After the emergency situation is lifted, the USV returns to a non-emergency state or sails directly to the sub-target point in an obstacle-free situation.

2. Cancellation of emergency situation

The cancellation of the emergency situation is not an inverse process relative to entering it. Otherwise the USVs will constantly enter and exit the emergency situation. To make sure that the cancellation of emergency situation is trustworthy, the judgment method is used as follows:

$$\lambda_{11}: \{(RO \geq d_2) \frown (TCP < 0)\} \quad (7)$$

In Eq. (7), d_2 indicates the arena of the obstacle boat, The TCPA indicates the time to the closest point of approach: a bigger TCPA indicates a safer situation while a negative TCPA indicates that the USV is kept away from the obstacle boat.

$$TCPA = |RO| \cos(|\gamma|)/|\Delta v|$$

where: $\gamma = \angle(RO, \Delta v)$which is the angle that the line α performs rotation to the line b through the minor arc, so it can be either positive or negative depending on whether the rotation is made in anticlockwise direction or clockwise direction. RO is a vector connecting the coordinates of the USV and the obstacle, Δv is the relative speed between the USV and obstacle ship.Eq. (7) expresses that the USV is outside the boat's area and the two ships are moving away from each other at the moment. The USV is temporarily safe, so the emergency situation could be cancelled.

After the cancellation of emergency situation, the USV returns to a non-emergency state, or sails directly to the sub-target point in an obstacle-free situation.

3. Emergency collision avoidance

In a more urgent situation, the above given VO algorithm may not function. Consequently, the decision-making process and adjustment layer are activated. In such case the USV is not allowed to adjust the course frequently because doing so may lead to misjudgement of the obstacle ship. On the one hand, the USV should work out an emergency avoidance strategy; on the other hand, its speed should be adjusted according to the strategy to be prepared for making a large angle change to avoid collision. To prepare a collision avoidance strategy, the following work is required:

(1) Determining the steering angle of the collision avoidance target, $\bar{\gamma}$ Setting the desired steering angle of the USV to $\bar{\gamma}$:

$$\bar{\gamma} = 30 \left\lceil \frac{\gamma}{30} \right\rceil \quad (8)$$

In this equation: $\lceil\ \rceil$ indicates rounding-up procedure, γ is the collision avoidance steering angle stipulated by International Regulations for Preventing Collisions at Sea (COLREGS), which may be taken as γ+ or γ– where γ+ is the angle required to turn to the direction required by COLREGS, and γ– is the angle in the opposite direction, as shown in Fig. 9. According to the time to the closest point of approach (TCPA), when the USV turns to γ, the USV does not collide with the obstacle. In the planning process, priority is given to γ+ considering the turning target and γ– the candidate target when γ+ does not work.

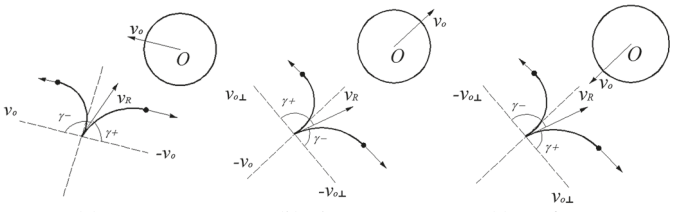

Fig. 9. Steering requirements for large rudder angle collision avoidance

$\boldsymbol{v}_{o\perp}$ is $\boldsymbol{v}_o$ rotated by 90° counterclockwise. $-\boldsymbol{v}_{o\perp}$ is $\boldsymbol{v}_o$ rotated by 90° in the opposite direction relative to $\boldsymbol{v}_{o\perp}$

According to Eq. (8), the angle values (30°, 60°, 90°, 120°, 150°, and 180°) can be selected as the steering targets. On the one hand, a sufficient margin for turning time is guaranteed; on the other hand, the data can be fitted by a polynomial previously obtained from the velocity vector database, this way the amount of data to be processed can be reduced. For ships that are difficult to manoeuvre, a more detailed range of angle values is required.

(2) Selecting the time function $t_{\bar{\gamma}}(V_x, \delta_y)$ required to obtain the angle $\bar{\gamma}$

According to the velocity vector database of the USV the polynomial function $t_{\bar{\gamma}}(V_x, \delta_y)$ acc. Eq. (4) is selected. This can be used to calculate the time required for the USV to make an emergency turn by $\bar{\gamma}$ angle at different initial values of the velocity V_x and rudder angle δ_y.

(3) Determining the constraints

Two requirements should be met by the USV to avoid obstacles safely in an emergency situation. First, the time of steering to safety angle should be less than the collision time. Second, the maximum heeling angle of the USV should be kept within the safe range. According to the two conditions, the feasible solution space for collision avoidance can be expressed in the form of the set Q:

$$Q: (V_m, \delta_n) = \{V_m \in V_i, \delta_n \in \delta_j \mid t_{\bar{\gamma}}(V_m, \delta_n) < TCPA, \phi_{\max}(V_m, \delta_n) < \phi_o\} \quad (9)$$

where ϕ_o is the maximum heeling angle in the state of safety, which is set to be 30° in this study. For example, when $\bar{\gamma} = 120°$, the dark area on the left side of Fig. 10 denotes the initial velocities and rudder angles that cannot meet the safe steering time, and the dark area on the right side denotes the initial velocities and rudder angles that cannot meet the maximum heeling angle within the safe range. The intermediate domain represents the set of feasible solutions which satisfy the initial velocity (V_m) and rudder angle (δ_n) conditions.

(4) Solving optimal collision avoidance speed and rudder angle in feasible solution space

The objective function of the collision avoidance strategy is:

$$\{V_{\bar{i}}, \delta_{\bar{j}} \mid \min f(V_{\bar{i}}, \delta_{\bar{j}}) = w_1 \mid V_{\bar{i}} - v_R \mid + w_2 \delta_{\bar{j}}\}, \quad (10)$$

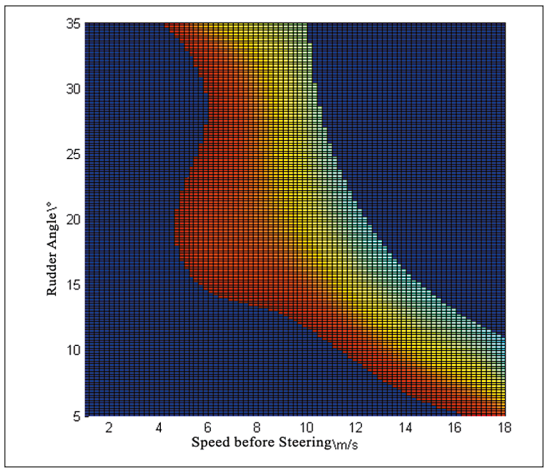

Fig. 10. Feasible solution determined by roll and turn time

meanwhile $(V_{\bar{i}}, \delta_{\bar{j}})$ Q,
where w_1 and w_2 are adjustable weights.

$$w_1 = \begin{cases} 1.2 & if\ v_0' > v_R \\ 0.8 & if\ v_0' \le v_R \end{cases},\ w_2 = 1$$

Eq. (10) shows that the solution with the smallest adjustment loss is selected from the feasible solution space Q, and thus, the USV can avoid collisions by changing its current motion as little as possible. For practical collision avoidance, in this study the two weighting values are set to prioritize change in rudder angle rather than that in speed. Moreover, when necessary, a deceleration is preferred over acceleration because speed increase requires the main engine to develop a higher rotational speed, which increases the power load of the USV, and to increase the speed is more difficult than to reduce it. Eq. (10) is solved by the particle swarm optimization.

(5) Obtaining an emergency collision avoidance track
Based on the mapping relations between the position coordinates of Eq. (5) and the initial velocity and rudder angle, the trajectory ($\boldsymbol{P}^*$) of the USV for emergency collision avoidance can be obtained by using the corresponding values of $(V_{\bar{i}}, \delta_{\bar{j}})$.

$$\boldsymbol{P}^* = [\boldsymbol{P}_{\bar{i},\bar{j},0}, \ldots, \boldsymbol{P}_{\bar{i},\bar{j},t}, \ldots, \boldsymbol{P}_{\bar{i},\bar{j},10}]^T$$

The collision avoidance process is shown in Fig. 11.

The USV path planning contains two parts, global path planning and local path planning. In global path planning, based on the electronic chart, the USV plans a global path which consists of a series of sub-goals for the USV to navigate as long as to arrive at the goal in the end. In the local path planning, the USV avoids all obstacles (boats) in the process of sailing from one sub-goal to the next. The collision avoidance process considered in this article belongs to the kind of local path planning. In each cycle, the USV calculates the process shown in the flowchart. At first, it checks the status λ_1, and, if TRUE is revealed it means that a crash happens and the collision avoidance process is failed. If λ_1 appears FALSE,

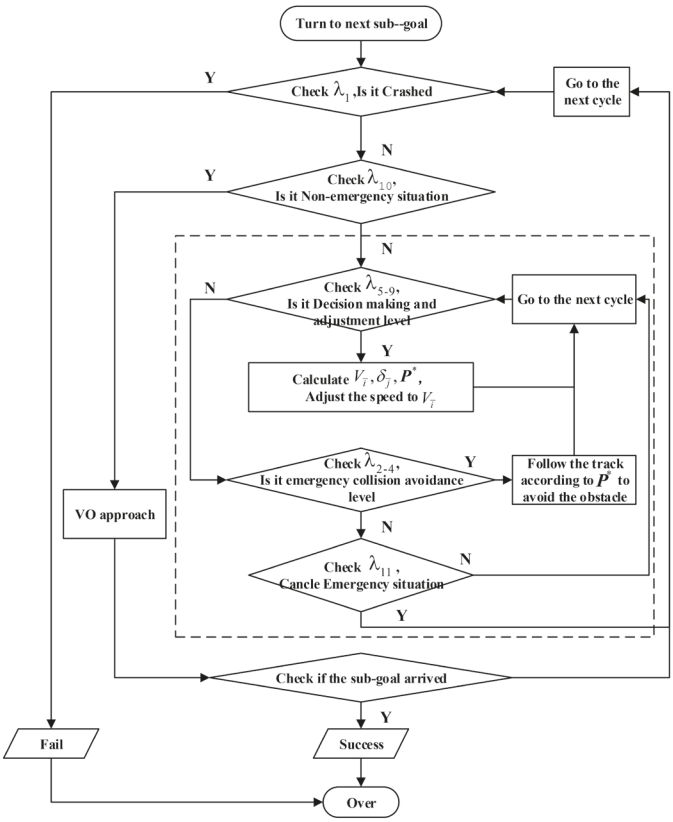

Fig. 11. Flowchart of collision avoidance process

the USV checks the status λ_{10} to make sure if it is in a non-emergency situation. TRUE means the USV is in a non-emergency situation, under this circumstance, to apply VO method is useful for the USV to avoid the obstacles. FALSE indicates that the USV is in an emergency situation. Under this condition, the expressions λ_2 through λ_9 are all checked to make sure which degree of danger is reached at each state and the level of corresponding collision avoidance strategy. In decision and adjustment making, $(V_{\bar{i}}, \delta_{\bar{j}})$ and the trajectory $\boldsymbol{P}^*$ of the USV is calculated for emergency collision avoidance, and then the operation goes to the next cycle. On the emergency collision avoidance level, the USV follows $\boldsymbol{P}^*$ to get away from the obstacle. If the status λ_{10} is correct, the emergency situation is cancelled. In the whole process, if a sub-goal arrived, the local path planning succeeds and the USV continues turning to the next sub-goal.

SIMULATION EXPERIMENT

To test the effect of the proposed method, we simulated the collision avoidance of a USV under a MATLAB environment. For better observation, we constructed a 3D view with the use of the Unity on the basis of MATLAB environment. The work was programmed in C# script where the calculation in MATLAB was linked to form a dynamic link library. The development platform is the Visual Studio. In all simulation models, the USV simulates real conditions, it is unaware of the following movement of obstacles and can only react based

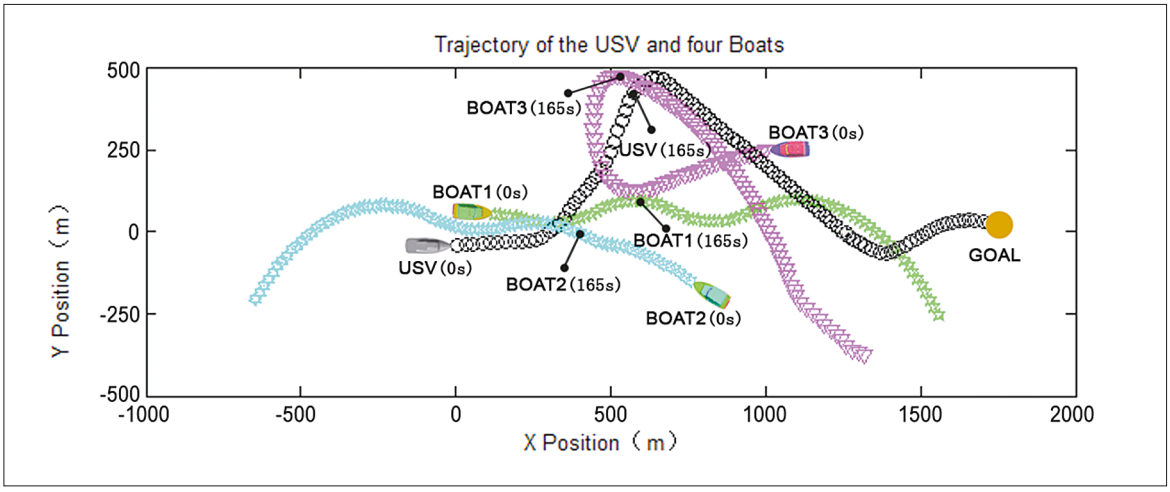

Fig. 12 Trajectories of the USV and three obstacle boats

on boats' current motion. The simulation cycle T is set to five seconds, which means that the movements of USV and obstacles are recorded every five seconds.

The USV represented by the black circle has an initial position of (0, -50) and an eastward velocity. The BOAT1 represented by the green pentacle is located at (80,50), and its velocity points to the east. The BOAT2 represented by the blue-green hexagon is located at (900,-200) and its velocity points to the northwest. The BOAT 3 represented by the magenta triangle is located at (1100,250), and its velocity points to the west. The obstacle ships move randomly. Fig. 12 shows the trajectories of the USV and the three ships. The movements of the obstacle ships cause interferences, but the USV could still safely avoid all the obstacles and successfully reach the end point.

In Fig. 12, the positions of the USV and the obstacles at 165 sec are shown, and Fig. 13 presents the moving relations between the ships at this moment. The magenta areas around BOAT3, marked from deep to light shade, represent the above mentioned D, DN, and DNN regions, respectively. The figure shows that at a particular moment, $\mathcal{C} \cap \mathcal{DNN} \neq \varnothing$, the BOAT3 is in λ_4 state. Thus, the USV should enter the execution layer and start emergency collision avoidance.

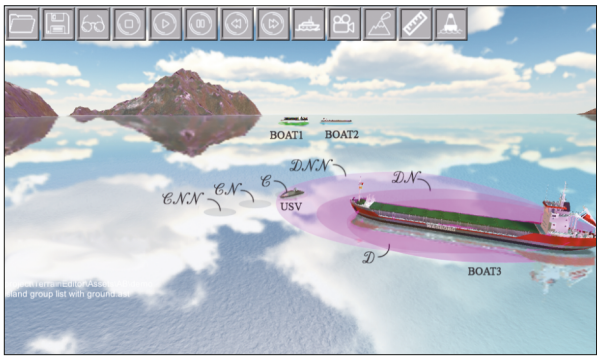

Fig. 13. Positional relationship between USV and obstacles at 165 sec

Fig. 14 shows the changes in encounter types when the USV meets the three obstacle ships. Throughout the process, BOAT2 maintains in a non-urgent situation, λ_{10}, with the USV, indicating that the VO algorithm is used for the USV to avoid BOAT2. BOAT1 and BOAT3 remain at λ_{10} state for a long time. During this period, the VO algorithm is also used by the USV. Subsequently, they enter an urgent situation, and the states change to λ_3 or even λ_2. This condition shows that the VO algorithm is no longer sufficient to guarantee the safety of the USV. Therefore, the USV starts using the emergency strategy to plan the trajectory and adjust the speed in the planning and adjustment layer ($\lambda_5 - \lambda_9$), and the steering has not yet been commenced. Thus, the emergency state is still under testing until it enters the execution layer ($\lambda_2 - \lambda_4$). At this time, the USV makes a large turn as planned to avoid collision. Consequently, the emergency state is quickly recovered, and then the USV briefly returns to the state λ_{10} but still uses the emergency collision strategy until it changes to state λ_{11}. After the emergency state is lifted, the USV jumps to the state λ_{10} and uses the VO algorithm for conventional collision avoidance planning.

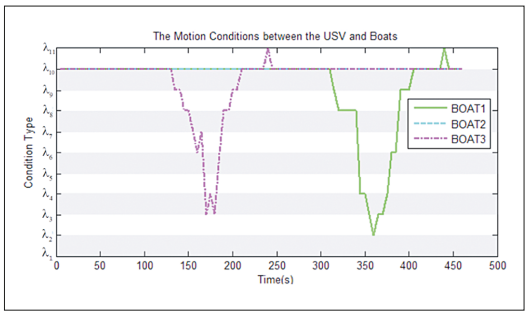

Fig. 14. The motion conditions between the USV and obstacle boats

Fig. 15 presents the curve of changing the heading angle and velocity of the USV during the collision avoidance process. The slanting direction and the speed are continuously and smoothly adjusted. In planning and adjusting layer, the speed of the USV is slowly adjusted and lowered in preparation for the execution layer that may appear later, indicating that the collision avoidance speed solved by the PSO algorithm is less than the current speed. When entering the executive level, the heading angle of the USV is quickly adjusted, indicating that a large steering to avoid collision is initiated. After the

emergency situation is lifted, the speed of the USV increases, and the VO algorithm is used to perform conventional collision avoidance process.

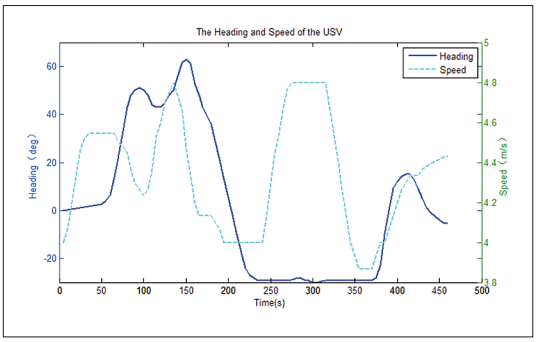

Fig. 15. The USV heading and speed in function of time

RECAPITULATION

This study proposes an emergency collision avoidance algorithm for USVs based on a motion ability database. The algorithm is aimed at addressing the inconsistency of the existing algorithm. It is proposed to avoid collision in emergency situations by sharp turning and treating the collision avoidance process as a part of the turning movement of USVs. In addition, the rolling safety and effect of speed reduction during the collision avoidance process are considered. Both the maximum heeling angle and the velocity vector are fitted into polynomials to perform quickly calculation when executing obstacle avoidance. After that, the time of steering to safety angle and the maximum heeling angle form two infeasible solution spaces, the obstacle avoidance problem turns to be an optimization problem in the feasible solution space. Moreover, the cancellation function of the emergency situation is proposed to avoid the USVs entering the emergency situation and exiting from it, over and over again. When a USV is in emergency collision avoidance process, the velocity vector and position vector are nonlinear. The existing algorithm is inconsistent or impossible to solve and does not consider the impact of speed drop on safety during heeling and steering. To address the problems, this study proposes a collision avoidance algorithm based on the USV motion ability database, which realizes emergency collision avoidance by sharp turning. First, a USV rotary motion simulation is conducted numerically and the motion ability database (with pre-steering initial velocity and steering rudder angle taken as independent variables) is obtained, including the heeling angle function for ensuring safety, which is used to determine the collision avoidance course. The velocity vector database and location database are used to determine the steering time function and collision avoidance trajectory. Second, a collision avoidance model is established for USVs and obstacles in emergency situations. By introducing the prediction period, the model is correlated with relative speed, which ensures the accuracy of emergency judgment. On the basis of the model, different emergency states are set and three layers of emergency avoidance process are formed, namely, the conventional collision avoidance layers using VO algorithm, the decision and adjustment layer for planning and speed adjustment, and the collision avoidance layer performing steering tasks. Third, the collision avoidance planning method in the decision and adjustment layer is determined. The expected steering angle is obtained by combining the COLREGS rule. The feasible solution space, with the initial velocity and rudder angle as the independent variables, is determined by combining the steering time and heel angle functions. On the basis of this solution space, the objective function is formed and solved by the PSO algorithm to obtain the optimal initial velocity and rudder angle. Then, the optimal trajectory can be obtained by referring to the corresponding position data. A simulation is conducted to confirm the validity of the proposed approach. The results of the simulation indicate that the proposed approach is valid and efficient.

ACKNOWLEDGMENT

This work is supported by the National Natural Science Foundation of China (Grant No. 51809203 and 51709214) and the Fundamental Research Funds for the Central Universities (WUT: 2019IVB011, 2017IVA008 and 2017IVA006).

REFERENCES

1. Campbell S., Naeem W., Irwin G.W.: *A review on improving the autonomy of unmanned surface vehicles through intelligent collision avoidance manoeuvre*. Annu. Rev. Control 2012, 36(23): pp. 267–283.

2. Simetti E., Turetta A., Casalino G.: *Towards the Use of a Team of USVs for Civilian Harbour Protection: the Problem of Intercepting Detected Menaces*, OCEANS 2010 IEEE – Sydney.

3. U.S.Dept. Homeland Security/U.S. Coast Guard; *Navigation rules*. Paradise Cay Publications, 2010.

4. Larson J., Bruch M., Halterman R., Rogers J., Webster R.: *Advances in Autonomous Obstacle Avoidance for Unmanned Surface Vehicles*. Space and Naval Warfare Systems Center, San Diego, CA., 2007.

5. Colito J.: *Autonomous mission planning and execution for unmanned surface vehicles in compliance with the marine rules of the road*, M.S. thesis, Dept. Aeronaut. Astronaut., Univ. Washington, Seattle, WA, US., 2007.

6. Choi, S., Yu, W.: *Any-angle path planning on non-uniform costmaps*. In: Proceedings of the IEEE International Conference on Robotics and Automation (ICRA), 2011: pp. 5615–5621.

7. Kim H., Park B., Myung H.: *Curvature path planning with high resolution graph for unmanned surface vehicle*. In: Proceedings of the Robot Intelligence Technology and Applications (RiTA), 2012: pp. 147–154.

8. Khatib, O.: *Real-time obstacle avoidance for manipulators and mobile robots*. Int. J. Robot. Res. 1986, 5: pp. 90–98.

9. Wang J., Wu X., Xu Z.: *Potential-based obstacle avoidance in formation control*. J. Control Theory Appl. 2008, 6: pp. 311–316.

10. Ge S., Cui Y.: *Dynamic motion planning for mobile robots using potential field method*. Auton. Robots 2007, 13: pp. 207–222.

11. Fiorini P., Shiller Z.: *Motion planning in dynamic environments using velocity obstalces*, Int. J. Robot, Res. 1998, 17(7): pp. 760–772.

12. Berg J., Lin M., and Manocha D.: *Reciprocal velocity obstacles for real-time multi-agent navigation*, Proc. IEEE Int. Conf. Robot. Autom., 2008: pp. 1928–1935.

13. Kluge B., 2004 Parssler: *Reflective navigation: Individual behaviors and group behaviors*, Proc. IEEE Int. Conf. Robot. Autom., 2004, 4: pp. 4172–4177.

14. Berg J., Patil S., Sewall J., Manocha D., and Lin M. C.: *Interactive navigation of multiple agents in crowded environments*, Proc. Symp. Interactive 3D Graphics Games, 2004, pp. 139–147.

15. Zhao Y.X., Li W., Shi P.: *A real-time collision avoidance learning system for Unmanned Surface Vessels*. Neurocomputing, 2016, 182: pp. 255–266.

16. Li W. F., Ma W. Y.: *Simulation on Vessel Intelligent Collision Avoidance Based on Artificial Fish Swarm Algorithm*. Polish Maritime Research, 2016, 23: pp. 138–143.

17. Lazarowska A.: *Swarm Intelligence Approach to Safe Ship Control*. Polish Maritime Research, 2015, 22(4): pp. 34–40

18. Soulignac M.: *Feasible and optimal path planning in strong current fields*. IEEE Trans. Robot. 2011, 27: pp. 89–98.

19. Isern G., Hernández, S. D., Fernández P. E., Cabrera G., Dominguez B., Prieto M. V.: *Path planning for underwater gliders using iterative optimisation*. In: Proceedings of the IEEE International Conference on Robotics and Automation (ICRA), 2011: pp. 1538–1543.

20. Yang Y., Wang S., Wu Z., Wang Y.: *Motion planning for multi-HUG formation in an environment with obstacles*. Ocean Engineering. 2011, 38: pp. 2262–2269.

21. Song L.F., Su Y.R., Dong Z.P.: *A two-level dynamic obstacle avoidance algorithm for unmanned surface vehicles*, Ocean Engineering, 2018, 170: pp. 351–360.

22. Song L.F., Chen Z., Xiang Z.Q.: *Error Mitigation Algorithm based on Bidirectional Fitting Method for Collision Avoidance of Unmanned Surface Vehicle*, Polish Maritime Research, 2018.

CONTACT WITH THE AUTHORS

Lifei Song
e-mail: songlifei@whut.edu.cn

Key Laboratory of High Performance Ship Technology
(Wuhan University of Technology)
Ministry of Education
Heping Avenue, 430063 Wuhan

School of Transportation
Wuhan University of Technology
Heping Avenue, 430063 Wuhan
China

Houjing Chen
e-mail: Hawking2006@sina.cn

Key Laboratory of High Performance Ship Technology
(Wuhan University of Technology)
Ministry of Education
Heping Avenue, 430063 Wuhan

China Ship Development and Design Center
Zhangzhidong Road, Wuhan
China

Wenhao Xiong
e-mail: 2569403518@qq.com

School of Transportation
Wuhan University of Technology
Heping Avenue, 430063 Wuhan
China

Zaopeng Dong
e-mail: dongzaopeng@whut.edu.cn

Key Laboratory of High Performance Ship Technology
(Wuhan University of Technology)
Ministry of Education
Heping Avenue, 430063 Wuhan

School of Transportation
Wuhan University of Technology
Heping Avenue, 430063 Wuhan
China

Puxiu Mao
e-mail: Puxiumao@usc.edu

University of Southern California
University Park Los Angeles
740–2311 Los Angeles
USA

Zuquan Xiang
e-mail: xiangzuquan@whut.edu.cn

Key Laboratory of High Performance Ship Technology
(Wuhan University of Technology)
Ministry of Education
Heping Avenue, 430063 Wuhan

School of Transportation
Wuhan University of Technology
Heping Avenue, 430063 Wuhan
China